



# Hydrogen bond interactions at the TiO<sub>2</sub> surface: Their contribution to the pH dependent photo-catalytic degradation of *p*-nitrophenol

Ronald Vargas, Oswaldo Núñez\*

Laboratorio de Fisicoquímica orgánica y química ambiental, Departamento de Procesos y Sistemas, Universidad Simón Bolívar, Apartado postal 89000, Caracas, Venezuela

## ARTICLE INFO

### Article history:

Received 12 January 2008

Received in revised form 15 October 2008

Accepted 19 October 2008

Available online 30 October 2008

### Keywords:

Langmuir isotherms

Langmuir–Hinshelwood (L–H)

*p*-Nitrophenol–TiO<sub>2</sub> pK<sub>a</sub>

Hydrogen bond interaction

TiO<sub>2</sub>

Adsorption equilibrium constant

Thermodynamic cycle

FTIR ATR

*p*-Chlorophenol

## ABSTRACT

We have obtained pK<sub>a</sub> values of *p*-nitrophenol–TiO<sub>2</sub> by measuring the adsorption equilibrium constants of *p*-nitrophenol (PNP) on the TiO<sub>2</sub> surface at different pH values. These values have been obtained from Langmuir isotherms and from a plot of 1/rate vs. 1/[PNP]<sub>0</sub> obtained during TiO<sub>2</sub> catalyzed solar light photo-degradation of PNP. Two limit equilibrium constants are readily obtained depending on the solution pH: at pH 5 at which the TiO<sub>2</sub> surface is mainly positively charged and at pH 8 when it is negatively charged. With these and other adsorption equilibrium constants and the PNP pK<sub>a</sub> value in solution, thermodynamic cycles are established in order to obtain the PNP pK<sub>a</sub> when it is adsorbed on positively charged, neutral and negatively charged TiO<sub>2</sub> surfaces. From these pK<sub>a</sub> values useful information on the PNP–TiO<sub>2</sub> interaction is readily obtained. For instance, the PNP nitro group interacts with the TiO<sub>2</sub> surface via a hydrogen bond, arising from the complex of water molecules with the Ti<sup>4+</sup> ions on its surface. The weaker the hydrogen bond donor, the stronger the oxygen nitro group basicity. Therefore, pK<sub>a</sub> changes on the phenolic hydroxyl group result from these interactions. Linear free energy correlations, maximum PNP adsorption capacity values (*Q*<sub>L</sub>) and FTIR ATR, spectrum support this proposal. A *k*<sub>obs</sub> vs. pH degradation profile of *p*-nitrophenol is also provided.

© 2008 Elsevier B.V. All rights reserved.

## 1. Introduction

For sometime we have been interested in finding favourable conditions for the degradation and mineralization of organic contaminants using heterogeneous photo-catalysis [1]. Among the methods currently available, TiO<sub>2</sub> photo-catalysis has been of great interest due to its efficiency [2] and its lower cost as compared, for instance, with degradation using the Fenton reagent [3–5]. In fact, we have been interested in optimizing the degradation and mineralization of contaminants from the oil industry [6,7] and fungicides and pesticides precursors [8]. In all cases, our main concern was to learn as much as possible from the reaction mechanism in order to improve reaction rates and selectivity toward contaminants. In order to pursue this objective, we have obtained rates and adsorption equilibrium constants from reactions under different initial conditions by using the Langmuir–Hinshelwood (L–H) relation (1), which, in the case of *p*-nitrophenol (PNP) as the organic contaminant, can be written as

$$r = \frac{d[\text{PNP}]}{dt} = \frac{kK[\text{PNP}]_0}{1 + K[\text{PNP}]_0} \quad (1)$$

where *r* is the PNP degradation rate, *k* ([ ] s<sup>−1</sup>) the apparent rate constant of the adduct phenol–TiO<sub>2</sub> degradation, *K* ([ ]<sup>−1</sup>) the adduct formation equilibrium constant and [PNP]<sub>0</sub>, the initial PNP concentration. Therefore, from a plot of 1/*r* vs. 1/[PNP], *K* can be obtained from the slope and *k* from the intercept. In cases in which the contaminant is present in solution as more than one species, for instance *p*-nitrophenol and its conjugate base (PNP<sup>−</sup>), the Langmuir–Hinshelwood rate expression is transformed to Eq. (2):

$$r = \frac{kK[\text{PNP}] + k'K'[\text{PNP}^-]}{1 + K[\text{PNP}] + K'[\text{PNP}^-]} \quad (2)$$

where *k'* and *K'* correspond to the degradation rate and the adsorption equilibrium constant of the PNP<sup>−</sup>–TiO<sub>2</sub> adduct. This equation can be readily simplified for the case in which 1 ≫ *K*[PNP] + *K'*[PNP<sup>−</sup>], where Eq. (2) is reduced to

$$v = kK[\text{PNP}] + k'K'[\text{PNP}^-] \quad (3)$$

When Eq. (3) is rewritten in terms of the total phenol concentration ([PNP]<sub>T</sub>), Eq. (4) is obtained:

$$r = \frac{kK[\text{H}^+]}{Ka + [\text{H}^+]} + \frac{k'K'Ka}{(Ka + [\text{H}^+])} \times [\text{PNP}]_T \quad (4)$$

\* Corresponding author. Tel.: +58 2129063317; fax: +58 2129063876.  
E-mail address: [onunez@usb.ve](mailto:onunez@usb.ve) (O. Núñez).

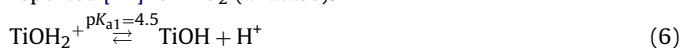
The last equation predicts that the observed rate constants,  $k_{\text{obs}} = r/[\text{phenol}]_T$ , can be obtained at each pH, to define a final  $k_{\text{obs}}$  vs. the pH sigmoid curve. In fact, we have obtained [9] such profiles for *p*-substituted phenols using a Hg lamp as light source.

Adsorption equilibrium constants can also be obtained from Langmuir isotherms according to Eq. (5):

$$q_e = \frac{Q_L K_L [\text{PNP}]}{1 + K_L [\text{PNP}]} \quad (5)$$

where  $q_e$  is the amount of PNP adsorbed,  $Q_L$  the maximum adsorption capacity of PNP on the  $\text{TiO}_2$  surface and  $K_L$  the Langmuir equilibrium constant.

However, the Langmuir equilibrium constants obtained may be different from the ones obtained from the Langmuir–Hinshelwood kinetic approach since, in the latter case, the  $\text{TiO}_2$  surface is illuminated, for instance with solar light. Therefore, the substrate interactions at  $\text{TiO}_2$  surface may change [10]. However, these changes are likely to be minimised at extreme pH since under these conditions the surface charge may then be mainly regulated by the  $\text{TiO}_2$   $\text{pK}_a$ . In fact, in Eqs. (6) and (7), the  $\text{pK}_a$  values of the two protonated  $\text{TiO}_2$  species are shown. Therefore, a zero point charge pH 6.25 value is obtained from Eq. (8). These values [11] correspond to  $\text{TiO}_2$  Degussa P25 (anatase:rutile 70:30%). A  $\text{pH}_{\text{zpc}}$  6.8 has been reported [12] for  $\text{TiO}_2$  (anatase):



$$\text{pH}_{\text{zpc}} = \frac{1}{2}(\text{pK}_{a1} + \text{pK}_{a2}) \quad (8)$$

An important aspect to be considered in  $\text{TiO}_2$ /solar UV light photo-degradation is the equilibrium constant for adsorption [13] of the PNP at the  $\text{TiO}_2$  surface, since according to Eq. (1), a stronger adsorption will be translated into a higher degradation rate, unless  $K[\text{PNP}] > 1$ . In such a case, the adsorption equilibrium will not affect the rate. Therefore, we are interested in exploring the characteristics of the PNP– $\text{TiO}_2$  association. In this regard we found the measurement of the  $\text{pK}_a$  value of the phenol at the  $\text{TiO}_2$  surface particularly useful, since any change of the phenol  $\text{pK}_a$ , as compared to its  $\text{pK}_a$  in water, will give us information about the PNP– $\text{TiO}_2$  interaction.

Moreover, since the charge on the  $\text{TiO}_2$  surface also changes with pH, the interaction of PNP with the positively charged, neutral and negatively charged  $\text{TiO}_2$  surface, should yield different  $\text{pK}_a$  values depending on the type of interaction. PNP is a very useful molecule in this regard due to the presence of the nitro group. In fact, it has been pointed out that, depending on the characteristics of the proton donor, the nitro group could form hydrogen bonds with  $-\text{X}-\text{H}$  molecules ( $\text{X} = \text{O}, \text{N}$  and  $\text{C}$ ) of different strengths and orientations [11]. This difference in strength is likely to be manifested by changed PNP– $\text{TiO}_2$   $\text{pK}_a$  values. Therefore, in this manuscript we deal with ways of finding those PNP– $\text{TiO}_2$   $\text{pK}_a$  values, the type of interaction between PNP and the  $\text{TiO}_2$  surface and its consequences for UV– $\text{TiO}_2$  catalyzed PNP degradation.

Thin-layer [14] electrochemical techniques have been used to take precise measurements of adsorbed amounts that define the orientations of adsorbed molecules by revealing the electrode (Pt) surface area required for formation of the adsorbed state. Photochemical measurement of phthalic acid adsorption on  $\text{TiO}_2$  film electrodes has also been reported [15]. FTIR spectroscopy [16] has also been used, for instance with phenols, to determine the type of interaction on the  $\text{TiO}_2$  surface. IR in diffuse reflectance mode (DRIFT) has been used [17] to study the chemisorption of phenols and acids on a  $\text{TiO}_2$  surface. The results presented herein are based on the adducts- $\text{pK}_a$  approach and provide additional and useful

information to the understanding of the  $\text{TiO}_2$  surface adsorption mechanism. Knowledge of the latter can be used to optimize reaction conditions for degradation.

## 2. Experimental

### 2.1. Reactants

Anatase, 99.9%  $\text{TiO}_2$  was obtained from Aldrich; *p*-nitrophenol, spectrophotometric grade, from Sigma and *p*-chlorophenol from Merck 98%.

### 2.2. Equipment

Irradiations were conducted using a LS 1000 UV solar light simulator from Solar Light Co., equipped with a xenon lamp of 1000 W and filters that simulate solar light intensities in the UVB and UVA (290–400 nm) regions. Radiation intensity was measured with a PMA 2100 radiometer from Solar Light Co. [PNP] kinetics were followed using a 8452A diode array Hewlett Packard (HP) UV–vis spectrophotometer. Millipore filtration equipment provided with cellulose and nitrocellulose 0.45  $\mu\text{m}$  filters and a digital pH meter, model P211, Hanna Instruments were also used.

FTIR ATR (Fourier transform infra red attenuated total reflection) spectra were taken on a Nicolet Magna-IR 750 serie II spectrometer with an ATR accessory with a ZnSe window and a software Omnic versión 4.1.

### 2.3. Langmuir isotherms

Langmuir isotherms, at 25 °C and pH 5.0, 6.0, 6.8 and 8.0, were obtained using 100 mg of  $\text{TiO}_2$  and PNP in the concentration range of 2–35 mg/L in a total volume of 100 mL of distilled water. The general procedure consisted of mixing 100 mg of  $\text{TiO}_2$  with the appropriate amount of PNP. To this mixture concentrated HCl or NaOH was added to obtain the desired pH. No buffer was used in order to avoid its competition for the active sites at the  $\text{TiO}_2$  surface. Once the desired pH was obtained, the mixture was stirred until the adsorption equilibrium was reached. This equilibrium was monitored by measuring the PNP absorbance of sample aliquots previously filtered using micro-pore filters on a UV–vis spectrometer. No changes in pH were observed during the experiments. In all cases equilibrium was reached in <5 h. The amount of PNP adsorbed on the  $\text{TiO}_2$  surface at each [PNP] was calculated from the difference between the total [PNP] and the [PNP] remaining in solution. [PNP] were obtained by using calibration curves (absorbance vs. [PNP]) at 318 nm (acid pH) or 402 nm (basic pH). Plots of [PNP] adsorbed on the surface, per gram of  $\text{TiO}_2$  added vs. the [PNP] in solution gives the Langmuir isotherms. From best fitting of the obtained experimental points to Eq. (5), the adsorption equilibrium constant ( $K_L$ ) and the maximum amount of PNP adsorbed ( $Q_L$ ) were obtained.

Additionally, Langmuir isotherms of PNP and *p*-chlorophenol were obtained at pH 3 and 40 °C. A molar adsorption coefficient of 1500  $\text{M}^{-1} \text{cm}^{-1}$  at 282 nm was obtained for *p*-chlorophenol.

The sample for the FTIR ATR spectrum was prepared by using 300 mg/kg of  $\text{TiO}_2$ , 300 mL of water solution at pH 3 and 20 mg/L of PNP. This mixture was stirred overnight. The solid was filtered and dried at room temperature for 12 h.

### 2.4. Langmuir–Hinshelwood (L–H) kinetic measurements

L–H kinetics were performed at 25 °C and at pH 6 or 8. In a typical experiment, 100 mg of  $\text{TiO}_2$  and 10–30 mg of PNP were added to 1 L of distilled water. To this solution NaOH or HCl were added

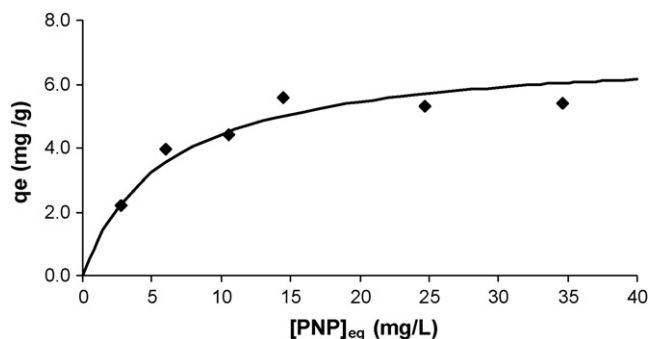


**Fig. 1.** Langmuir isotherm for the adsorption of PNP on the TiO<sub>2</sub> surface at pH 5. Solid line: best fitting of the experimental points using Eq. (5):  $Q_L = 7.07$  mg/g and  $K_L = 0.14$  L/mg.

to adjust pH to the desired value. This solution was irradiated with simulated UVB and UVA light ( $22 \mu\text{W}/\text{cm}^2$ ) while stirred mechanically. Reaction aliquots were taken at different reaction times. These aliquots were filtered and their [PNP] was obtained by measuring the PNP absorbance at 318 nm or 402 nm in an UV-vis spectrometer. The absorbance values were transformed into the actual [PNP] from calibration curves previously prepared. The rates ( $r$ ) at each [PNP] were obtained from the initial slope of a [PNP] vs.  $t$  plot. From a plot of  $1/r$  vs.  $1/[\text{PNP}]_0$  the  $k$  and  $K$  values of Eq. (1) were obtained. Alternatively, the PNP degradation  $k_{\text{obs}}$  values were obtained from the slope of a plot of  $\ln [\text{PNP}]$  vs.  $t$ .

Additionally, L–H kinetics were measured for PNP and *p*-chlorophenol at pH 3 and 40 °C. For *p*-chlorophenol, a calibration curve of absorbance at 282 nm vs. [*p*-chlorophenol] was used to obtain the initial rates and the  $k_{\text{obs}}$  value.

### 2.5. Accumulated irradiation and quantum yield

The accumulated radiation ( $I$ ) at 300–387 nm, and the quantum yield ( $Q$ ), were calculated as follows: a direct UV radiation (300–387 nm) of  $22 \text{ W}/\text{m}^2$  that corresponds to  $6 \times 10^{-5}$  einstein/(m<sup>2</sup> s) ( $6 \times 10^{-9}$  einstein/(cm<sup>2</sup> s)) was used. For a solar simulator cannon diameter of 14 cm the light intensity per unit of time is:  $6 \times 10^{-9}$  einstein/(cm<sup>2</sup> s)  $\times 3.14 \times 49 = 9.2 \times 10^{-7}$  einstein/s ( $5.52 \times 10^{-5}$  einstein/min).

From this value the quantum yield can be obtained from:  $Q = (dI/dt \times 1 \text{ L})/I = 5.89 \times 10^{-4} \text{ mmole}/\text{min} / 5.22 \times 10^{-2} \text{ meintein}/\text{min} = 0.01$ , where  $dI/dt$  is the PNP degradation rate (a value of  $8 \times 10^{-2} \text{ mg}/\text{L}$  is used in the calculation), 1 L is the solution volume used and  $I$  the light intensity. In this calculation of the quantum yield the total incident light has not been corrected by the fraction that is actually absorbed by the TiO<sub>2</sub>. This fraction has been determined, ca. 0.1, via spectrophotometric integrating sphere technique [18]. When this fraction is taken into account, a quantum yield of 0.1 is obtained. This quantum yield is in agreement, for instance, with values obtained [18] for phenol.

## 3. Results

The Langmuir isotherm for the adsorption of PNP on the TiO<sub>2</sub> (anatase) surface at 25 °C and pH 5 is shown in Fig. 1. The corresponding Langmuir isotherm parameters at 25 °C and pH 5, 6, 8 and 8 are shown in Table 1 (second and third columns). In this table the Langmuir isotherm parameters for PNP at pH 3 and 40 °C are also shown.

In Fig. 2, a Langmuir–Hinshelwood plot of  $1/\text{rate}$  vs.  $1/[\text{PNP}]_0$  at pH 8 and 25 °C is shown and in Fig. 3, the corresponding plot of  $\ln [\text{PNP}]$  vs.  $t$  is shown. Similar plots are obtained at pH 6 (not shown). In

**Table 1**

Langmuir isotherm experimental values for the PNP adsorption on the TiO<sub>2</sub> (anatase) surface at different pH values.

pH	$Q_L$ (mg/g)	$K_L$ (L/mg)	$K_{LH}$ (L/mg)	$k_{LH}$ (min <sup>-1</sup> mg/L)	$k_{\text{obs}}$ (min <sup>-1</sup> )
3 <sup>a</sup>	7.47	0.13	0.10(0.012 <sup>b</sup> )	0.19(0.83 <sup>b</sup> )	0.028(0.012 <sup>b</sup> )
5	7.07	0.14(−6.4) <sup>c</sup>			
6	7.79	0.10	0.17	0.087	0.015
6.8	16.4	0.13			
8	26.9	0.07	0.09	0.26	0.023

The experimental Langmuir–Hinshelwood (L–H) values and the  $k_{\text{obs}}$  values at [PNP] = 5 mg/L at pH 6, 8 and 3 (40 °C) are also shown.

<sup>a</sup> Experiments performed at 40 °C.

<sup>b</sup> *p*-Chlorophenol values.

<sup>c</sup>  $\Delta\Delta G^\circ$  (kJ mol<sup>-1</sup>) value at 25 °C calculated from  $\Delta\Delta G^\circ = -RT \ln K_L(\text{PNP})/K_L(\text{phenol})$  [15].

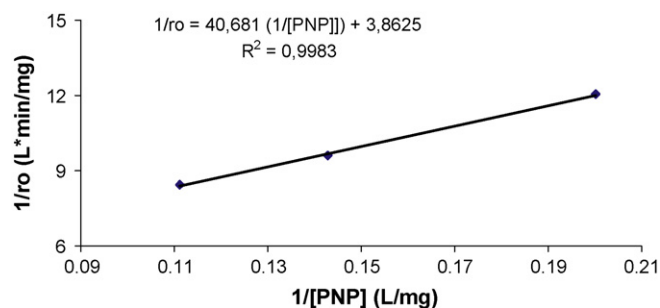


**Fig. 2.** Langmuir–Hinshelwood (L–H) plot of  $1/\text{rate}$  vs.  $1/[\text{PNP}]_0$  at pH 8; 100 mg TiO<sub>2</sub>. Lamp intensity:  $22 \mu\text{W}/\text{cm}^2$ .

Table 1 (the fourth column to the last one), the corresponding  $k$ ,  $K$  and  $k_{\text{obs}}$  values obtained from the last plots at pH 6 and 8, can be seen. In this table, the corresponding Langmuir–Hinshelwood parameters for PNP and *p*-chlorophenol at pH 3 and 40 °C are also shown.

FTIR ATR spectrum of the surface-modified TiO<sub>2</sub> with PNP is shown in Fig. 8.

## 4. Discussion

As shown in Table 1, the adsorption equilibrium constants obtained kinetically from Eq. (1) in the catalyzed photodegradation of PNP at pH 6, 8 and 3 (40 °C) (the fourth column) are quite similar to those obtained from the Langmuir isotherms (the third column) in which no light was used during the adsorption. Therefore, the presence of light does not appear to modify the PNP–TiO<sub>2</sub> interaction.

Under pH 7, most of the PNP ( $\text{p}K_a = 7.14$ ) exists as its protonated form so that the  $K$  values obtained at pH 3, 5 and 6, represent

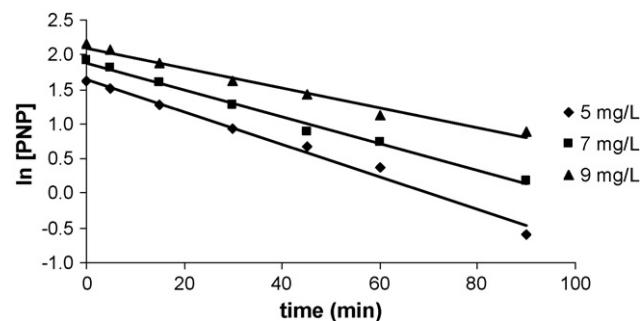


**Fig. 3.** Plot  $\ln [\text{PNP}]$  vs. time at three different  $[\text{PNP}]_0$ . In agreement with Eq. (1), the  $k_{\text{obs}}$  values depend on the  $[\text{PNP}]_0$ . In fact, at 5, 7 and 9 mg/L the  $k_{\text{obs}} = -\text{slopes} = 0.023$ , 0.019 and 0.014 min<sup>-1</sup>.

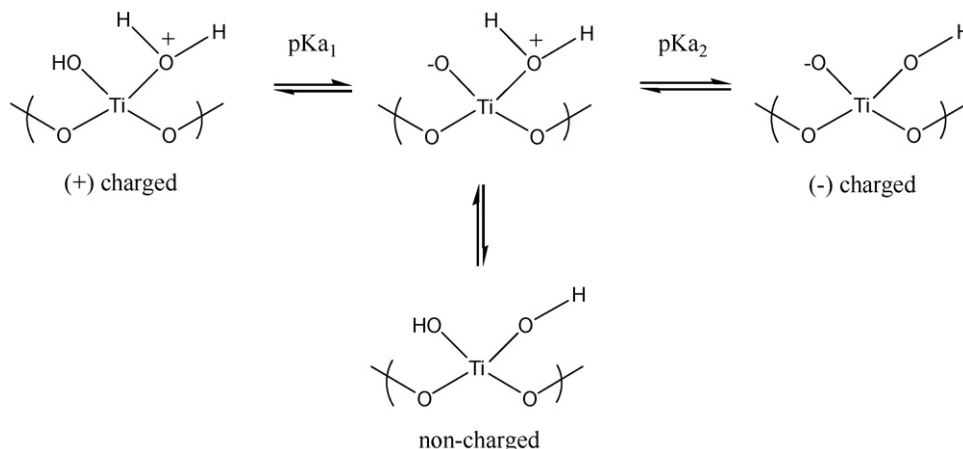


**Fig. 4.** Water and OH interactions with Ti (IV) at the  $\text{TiO}_2$  surface. As shown (+) charged, uncharged and/or (–) charged species may act as proton donors to form hydrogen bonds.

**Table 2**

PNP and  $\text{PNP}^-$  adsorption equilibrium values for their interaction with positively (+) charged, uncharged and (–) charged  $\text{TiO}_2$  surface.

	$\text{TiO}_2$ surface		
	(+) Charged	Neutral	(–) Charged
PNP, $K_1$ (L/mg)	0.14 <sup>a</sup>	0.06 <sup>b</sup>	0.02 <sup>b</sup>
$\text{PNP}^-$ , $K'_1$ (L/mg)	0.21 <sup>b</sup>	0.13 <sup>a</sup>	0.07 <sup>a</sup>
PNP, $\text{p}K_a$	6.9 <sup>c</sup>	6.8 <sup>c</sup>	6.6 <sup>c</sup>

PNP– $\text{TiO}_2$   $\text{p}K_a$  values, obtained using Scheme 1 thermodynamic cycle, are also shown. In water,  $\text{PNP}$   $\text{p}K_a = 7.1$ .

<sup>a</sup> Experimental values.

<sup>b</sup> Obtained from linear regression of the experimental points (see text).

<sup>c</sup> Obtained from Eq. (8):  $\text{p}K_a = 7.14 + \log K - \log K'$ .

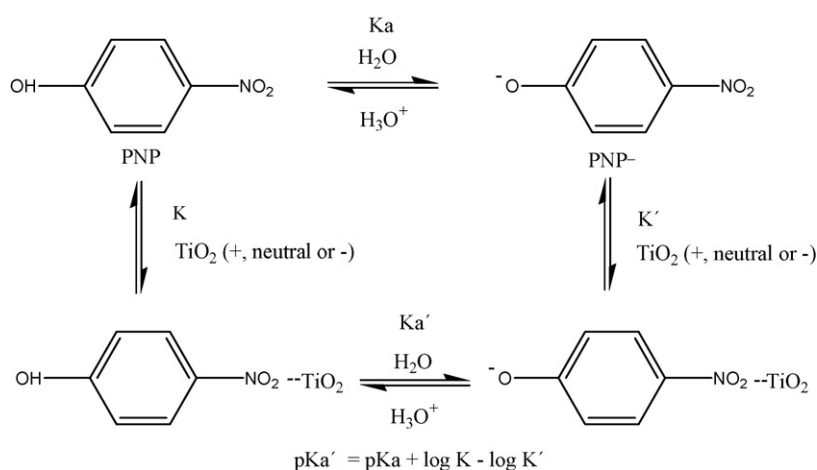
the PNP interaction with the  $\text{TiO}_2$  surface. These equilibrium constants are similar but different since when pH is increased, the  $\text{TiO}_2$  surface becomes less positively charged (see Eqs. (6) and (7)). By linear regression of the two points at 25 °C (pH 5 and 6), the interaction of PNP with the  $\text{TiO}_2$  surface at pH 6.8 and 8.0 can be estimated. These values are shown in Table 2. The experimental  $K$  value (0.13) obtained at pH 6.8 is double that estimated based on only the PNP– $\text{TiO}_2$  interaction. Therefore,  $\text{PNP}^-$  (PNP conjugated base) may also be contributing as adsorbed species. It has been previously suggested [19] that both  $\text{PNP}^-$  species might participate in the adsorption at the  $\text{TiO}_2$  surface and in the photo-degradation

process. In fact, since  $\text{PNP} = \text{PNP}^-$  interconversion is fast compared to the rate at which the adsorption equilibrium is established, the observed high adsorption constant may be attributed to the interaction of the  $\text{PNP}^-$  form with the neutral  $\text{TiO}_2$  surface. In the same table, the experimental  $K$  equilibrium adsorption at pH 8 is shown. Since at this pH PNP exists mainly as its  $\text{PNP}^-$  form, this  $K$  value corresponds to the adsorption of  $\text{PNP}^-$  on the negatively charged  $\text{TiO}_2$  surface. By using this value and the one estimated for the  $\text{PNP}^-$ – $\text{TiO}_2$  interaction, the  $\text{PNP}^-$  adsorption with the positively charged (pH 5)  $\text{TiO}_2$  surface is found by linear regression. This value is also shown in Table 2.

With PNP and  $\text{PNP}^-$  adsorption equilibrium values in Table 2, three thermodynamic cycles can be established. These cycles take into account the interaction of the PNP species with the positively, neutral (uncharged) and negatively charged  $\text{TiO}_2$  surface. Moreover, from each of these cycles the  $\text{p}K_a$  values for the PNP– $\text{TiO}_2$  adducts can be found (see Scheme 1) from the thermodynamic relations:

$$\text{p}K_a \text{ adduct} = \text{p}K_a + \log K - \log K' \quad (9)$$

The three  $\text{p}K_a$  values obtained are shown in Table 2. In the three cases, the  $\text{p}K_a$  values are lower than the  $\text{p}K_a$  of PNP in water (7.14). This tendency can be explained in terms of the PNP interaction with the  $\text{TiO}_2$  surface through the PNP nitro group. In fact, in the PNP molecule it is the site with higher charge density. Moreover, it has



**Scheme 1.** Thermodynamic cycle showing the interaction of PNP and  $\text{PNP}^-$  with the positive (+), neutral and negatively (–) charged  $\text{TiO}_2$  surface. Using the corresponding  $K$  and  $K'$  values of Table 2, and the  $\text{p}K_a$  of PNP in water (7.14), the  $\text{p}K_a'$  values are obtained. These values correspond to the PNP– $\text{TiO}_2$  adducts acidity constants.



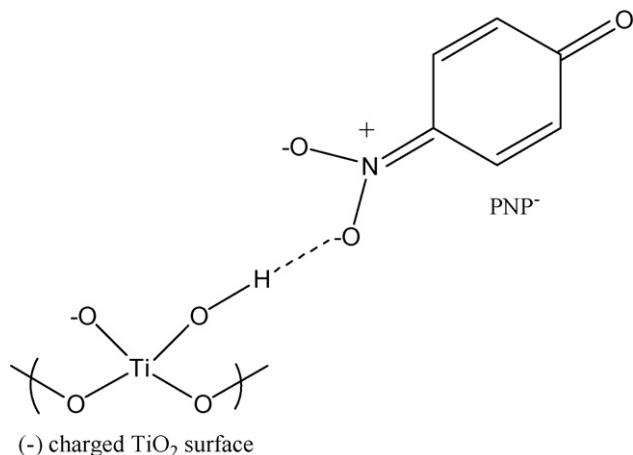


**Fig. 5.** Hydrogen bond interaction between the Ti–OH donor and the proton acceptor  $\text{PNP}^-$  at pH 8.

been pointed out that the nitro group forms hydrogen bond with  $-\text{X}-\text{H}$  species and that the strength of that hydrogen bond depends on the electron density on the nitro group acceptor and the acidity of the  $-\text{X}-\text{H}$  donor. Since the donors at the  $\text{TiO}_2$  surface are  $-\text{H}_2\text{O}^+$  or  $-\text{OH}$  that act as ligands on the Ti (IV) (see Fig. 4), a change in the interaction strength is expected. Furthermore, the nitro group donor also changes in going from  $\text{PNP}$  to  $\text{PNP}^-$  since, in the last case, there is more negative charge density delocalized at the nitro group through its resonance form. Therefore, the hydrogen bond acceptor becomes stronger and in turn, the hydrogen bond interaction. Thus, the strongest interaction in the  $\text{PNP}^-$ – $\text{TiO}_2$  adduct is expected to occur when  $\text{PNP}^-$  interacts with the positively charged  $\text{TiO}_2$  surface (low pH, see Fig. 4 and Table 2). However, the weakest, is not at high pH since a strong acceptor (e.g. like  $\text{PNP}^-$ ) can still form a hydrogen bond with  $-\text{OH}$  on the  $\text{TiO}_2$  surface (see Fig. 5). The last statement is in agreement with the experimental and estimated adsorption equilibrium constants and estimated  $\text{pK}_a$  values reported in Table 2.

We have discounted the  $\text{PNP}$  interaction with  $\text{TiO}_2$  surface through the  $-\text{OH}$  group since this interaction has been reported [16] for resorcinol, phenol and cresols and the obtained  $K_L$  values are one order of magnitude lower than the reported in this work. Only in the case of catechol (0.06 mg/L) is the interaction of the same order of magnitude as the  $\text{PNP}$  values but still lower than the values reported in Table 2. Moreover, *ab initio* molecular calculations [11] at the MP2/TZV level show directional hydrogen bond interaction between the nitro group and water with potential wells with depths greater than  $4 \text{ kJ mol}^{-1}$ . In agreement with these calculations, the  $\Delta\Delta G^\circ$  values, obtained from the  $K_L(\text{PNP})/K_L(\text{phenol})$  at pH 5, is  $6.4 \text{ kJ mol}^{-1}$  (see column 3, Table 1). The  $K_L(\text{phenol})$  value has been reported [16] previously. In fact, from FTIR studies it has been concluded that phenol interacts with the  $\text{TiO}_2$  surface through the phenol oxygen and does not form a hydrogen bond with water molecules at the surface as  $\text{PNP}$  does. Therefore, the  $K_L(\text{PNP})/K_L(\text{phenol})$  ratio and the associated  $\Delta\Delta G^\circ$  value, may be considered as the excess of free energy stabilization due to the hydrogen bond formed between the water molecule at the  $\text{TiO}_2$  surface and the  $\text{PNP}$  nitro group.

We found it interesting to correlate our results with the results published [20] on the Hammett study on the  $\text{TiO}_2$ -catalyzed photooxidation of para-substituted phenols. In that manuscript,  $K_{\text{LH}}$  are plotted vs. Hammett parameter  $\sigma_1$ . Two kind of straight lines are found: One with a negative slope (all substituents, including  $\text{X}=\text{H}$  (phenol)) and the other with a positive slope for  $\text{X}=\text{halogens}$ . Therefore, they suggest different adsorption modes

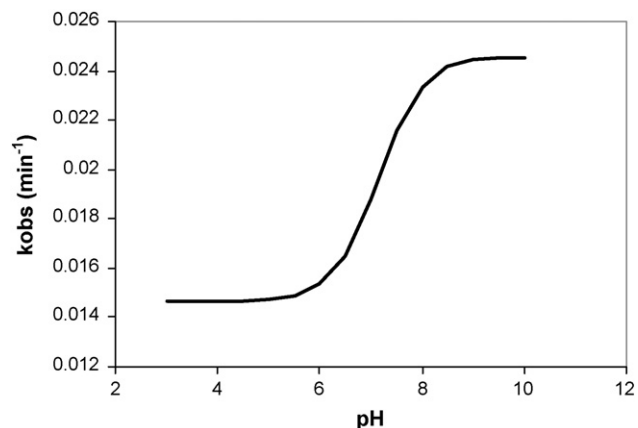


**Fig. 6.** Plot  $k_{\text{obs}}$  vs. pH for  $\text{PNP TiO}_2$  photo-degradation according to Eq. (4). Experimental  $kK$  and  $k'K'$  at pH 6 and 8, respectively, were used to obtain the profile.

for the halogenated and nonhalogenated para-monosubstituted phenols; *p*-nitro phenol is not included in the study. Therefore, we have measured  $K_L$  and  $K_{\text{LH}}$  values under the same conditions as the one reported [20]: pH 3 and  $40^\circ\text{C}$ . To verify that this result is comparable to the previously reported [20], we have also measured, under the mentioned conditions,  $K_{\text{LH}}$  value for *p*-chlorophenol. As shown in Table 1, the  $K_{\text{LH}}$  for the last compound is very similar ( $1609 \text{ M}^{-1}$ ) to the one previously reported [20] ( $1600 \text{ M}^{-1}$ ). Therefore, we feel confident to add the  $\text{PNP } K_{\text{LH}}$  value obtained in this work (Table 1) to the reported [20] Hammett correlation. This  $\text{PNP } K_{\text{LH}}$  high value ( $0.10 \text{ L/mg}$  ( $13,900 \text{ M}^{-1}$ ) at pH 3) does not fit at all the non-halogenated para substituent in which the constants decrease with  $\sigma_1$ ; however, it fits better the halogenated ones in which a positive slope is found. This result supports our proposal of a hydrogen bond interaction with the nitro group. It is quite probable that a similar mechanism is operating with the halogen substituents, although through a weaker hydrogen bond. In fact, molecular calculations [21] performed on *p*-halophenol show that in the case of *p*-fluorophenol, an important density charge is developed on the F atom. It is also quite important that the reactivity order ( $k \times K$ ) of *p*-halophenols is quite higher than other *p*-substituted

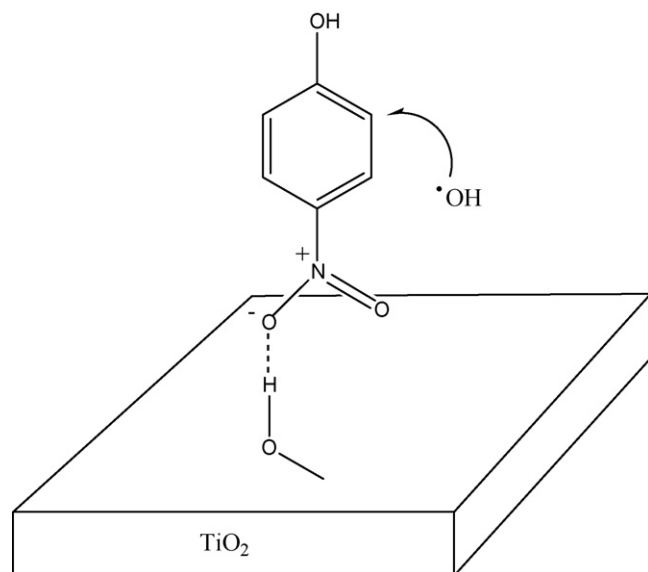


**Fig. 7.**  $\text{PNP}$  is adsorbed perpendicularly to the  $\text{TiO}_2$  surface and the  $\text{OH}$  radical attack occurs on carbon 2 or 6 as depicted.

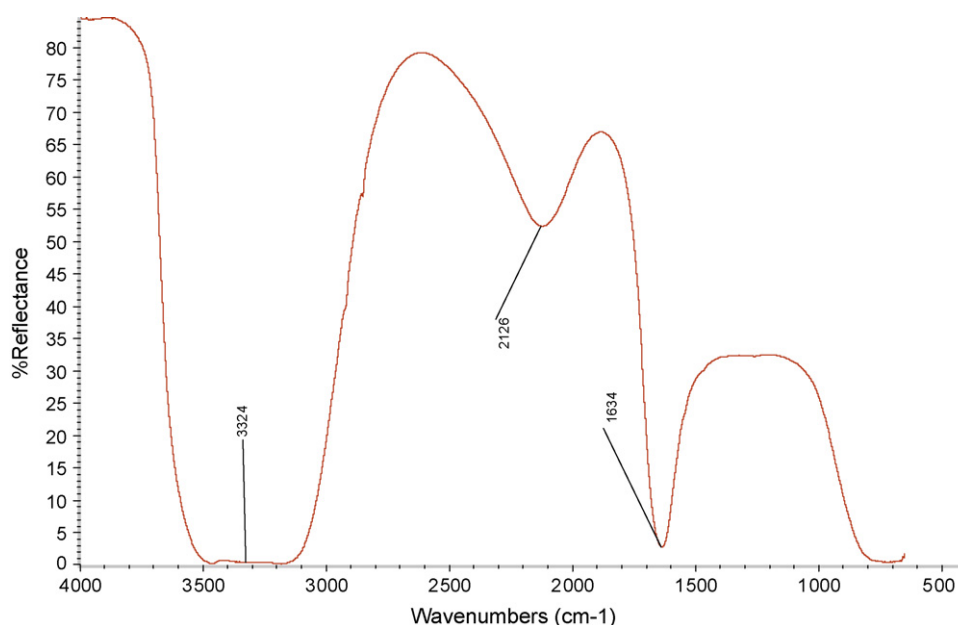


Fig. 8. FTIR ATR spectrum of  $\text{TiO}_2$ -PNP.

phenols except for *p*-nitrophenol that has the highest reactivity. From the mechanistic point of view, we could propose that the radical OH generated on the  $\text{TiO}_2$  surface interacts easily with the *p*-substituted phenol adsorbed perpendicularly at the  $\text{TiO}_2$  surface, as shown in Fig. 7, than with the one adsorbed parallel via  $\pi$  interaction. Although a perpendicular interaction as the one shown in Fig. 7 is certainly operating at high pH, at low pH an additional interaction between the hydrogen-bonded PNP may be acting between the aromatic  $\pi$  electrons and the positive charged  $\text{TiO}_2$  surface. This interaction may twist the molecule from the perpendicular position toward a nearly planar one. This argument is supported by the  $Q_L$  values reported in Table 1 where at low pH these values are significantly lower than at high pH. That is, at low pH there is less space on the surface to adsorb PNP molecules than at high pH, although the adsorption is stronger at low pH than at high pH.

A profile of  $k_{\text{obs}}$  vs. pH for the solar light  $\text{TiO}_2$  catalyzed degradation of PNP is shown in Fig. 6. This profile has been obtained using Eq. (4) and the experimental values of  $Kk$  and  $K'k'$  obtained at pH 6 and 8, respectively. Degradation is faster at higher pH due to the relative efficiency of the  $\text{PNP}^-$ - $\text{TiO}_2$  interaction and the high  $k$  value (efficient degradation rate constant) at high pH due to the increase in the  $[\text{OH}^\bullet]$ . In fact, the  $k_{\text{LH}}$  value at pH 8 is considerably higher than the one at pH 6. Therefore, besides the additionally formed hydroxyl radicals, the electron deficiency on the aromatic ring, due to the electron delocalization toward the nitro group (see Fig. 5), may also be contributing to the high observed rates at this pH.

A mechanism of the photodecomposition of PNP at the  $\text{TiO}_2$  surface is proposed in Fig. 7. The OH radical formed at the surface, as a consequence of water molecule oxidation, diffused to the perpendicularly adsorbed PNP molecule to produce the dihydroxycyclohexadienyl radical to probably yield *p*-nitrocatechol, an intermediate detected [22] in the electrophilic addition of hydroxyl radicals. This attack is favoured as compared to a parallel adsorbed molecule due not only to the charge density at the aromatic ring, but also statistically since only one molecule face is available for the electrophilic radical attack when the molecule is attached in a planar manner.

Finally, from the FTIR ATR of  $\text{PNP-TiO}_2$  adduct shown in Fig. 8, three main bands are detected. A broad one at  $3324\text{ cm}^{-1}$  typical of

a hydrogen bonded OH group ( $\text{TiO}_2$ ), an aromatic one at  $2126\text{ cm}^{-1}$  and a band at  $1634\text{ cm}^{-1}$  that could be attributed to the nitro group bands that have been blue shifted due to the hydrogen bond formed with the  $\text{TiO}_2$ -OH groups. Two bands at ca.  $1537$  and  $1360\text{ cm}^{-1}$  are the typical asymmetric and symmetric stretch bands of the nitro group. However shifts of these bands (approaching each other) have been observed [23] due the coordination of the nitro group to cations. It is then possible that the observation of only one band at  $1634\text{ cm}^{-1}$  is due to the overlapping of these band that are further blue shifted due to the strong hydrogen bond formed between the nitro group and the  $\text{TiO}_2$ -OH groups at its surface.

## 5. Conclusions

The  $\text{pK}_a$  of *p*-nitrophenol adsorbed on three types of  $\text{TiO}_2$  surfaces: positively, neutral and negatively charged, have been estimated from experimental PNP adsorption equilibrium constants measured by using the Langmuir isotherm. These equilibrium constants are quite similar to those obtained kinetically from the Langmuir-Hinshelwood approach. Therefore, it appears that there is no important perturbation of the  $\text{PNP-TiO}_2$  interaction when the  $\text{TiO}_2$  surface is illuminated with solar UV light.

PNP is more acidic when adsorbed at any of the above  $\text{TiO}_2$  surfaces than in water. PNP interaction at the  $\text{TiO}_2$  surface occurs through the PNP nitro group which forms a hydrogen bond with  $\text{Ti-H}_2\text{O}$  complexes at the  $\text{TiO}_2$  surface. This interaction becomes stronger when the electron density on the nitro group and the acidity of the donor (water molecules) are increased. Therefore, even at high pH, the  $\text{PNP}^-$  adsorption at the negatively charged  $\text{TiO}_2$  surface is relatively strong ( $K_L = 0.07\text{ L/mg}$ ).

The  $k_{\text{obs}}$  vs. pH profile predicts a more efficient PNP photo-catalytic degradation at  $\text{pH} > 8$ . For environmental water decontamination purposes, degradation at  $\text{pH} > 8$  can be achieved at a rate  $= 0.023\text{ min}^{-1}$   $[\text{PNP}]_T$ , at  $[\text{PNP}]_T < 10\text{ mg/L}$ .

## Acknowledgements

We acknowledge the Environment Management Unit (UGA) at Simon Bolivar University for financial support. We are also grate-

ful to the Royal College of Surgeons in Ireland and in particular to Professor Kevin Nolan for his hospitality and support during the sabbatical of one of the authors (ON) during which part of this manuscript was written.

## References

- [1] M.A. Fox, M.T. Dulay, *Chem. Rev.* 93 (1993) 341–357.
- [2] D.F. Ollis, E. Pelizzetti, N. Serpone, *Photocatalysis: Fundamentals and Applications*, Wiley-Interscience, New York, 1989.
- [3] H.J.H. Fenton, *J. Chem. Soc.* 65 (1894) 899.
- [4] C. Walling, *Acc. Chem. Res.* 8 (1975) 125.
- [5] R. López, O. Núñez, F. Morales, C. Calderón, W. Liewald, *Acta Cient. Venez.* 50 (1) (1999) 75.
- [6] A. Núñez, G. Pardo, O. Núñez, Chapter: Oil Industry Liquid Waste Treatment. Our Laboratory Experience. *Química Sustentable en Universidades Latinoamericanas*. Ed. Universidad Nacional del Litoral (UNL). Argentina, 2003.
- [7] N. Barrios, P. Sívov, D. D'Andrea, O. Núñez, *Int. J. Chem. Kinet.* 37 (7) (2005) 414–419.
- [8] I. Kuehr, O. Núñez, *Pest. Manag. Sci.* 63 (5) (2007) 491–494.
- [9] M.A. Martínez, A. Núñez, R. López, F. Morales, O. Núñez, *Acta Cient. Venez.* 50 (1) (1999) 81–86.
- [10] M.R. Hoffmann, S.T. Martin, W. Choi, D.W. Bahenemann, *Chem. Rev.* 95 (1995) 69–96.
- [11] J.M.A. Robinson, D. Philp, K.D.M. Harris, B.M. Kariuki, N. J. *Chem.* 24 (2000) 799–806.
- [12] J. Zhao, K. Wu, T. Wu, H. Hidaka, N. Serpone, *J. Chem. Soc. Faraday Trans.* 94 (5) (1998) 673–676.
- [13] M.R. Hoffmann, S.T. Martin, W. Choi, D.W. Bahnemann, *Chem. Rev.* 95 (1995) 69–96.
- [14] M. Soriaga, A. Hubbard, *J. Am. Chem. Soc.* 104 (10) (1982) 2735–2742.
- [15] J. Dianlu, Z. Huijun, S. Ging, J. Richard, W. Geoffrey, *J. Photochem. Photobiol. A: Chem.* 156 (1–3) (2003) 201–206.
- [16] J. Araña, E. Pulido Melian, V.M. Rodríguez López, J.A. Peña Alonso, M. Doña Rodríguez, O. González Díaz, J. Pérez Peña, *J. Hazard. Mater.* 146 (2007) 520–528.
- [17] D. Robert, S. Parra, C. Pulgarin, A. Krzton, J.V. Weber, *Appl. Surf. Sci.* 167 (2000) 51–58.
- [18] A. Salinaro, A.V. Emeline, J. Zhao, H. Hidaka, V.K. Ryabchuk, N. Serpone, *Pure Appl. Chem.* 71 (2) (1999) 321–335.
- [19] V. Augugliaro, L. Palmisano, M. Schiavello, A. Sclafani, L. Marchese, G. Martra, F. Miano, *Appl. Catal.* 69 (2) (1991) 323–340.
- [20] K.E. ÓShea, C. Cardona, *J. Org. Chem.* 59 (17) (1994) 5005–5009.
- [21] W. Zierkiewicz, D. Michalska, B. Czarnick-Matusiewicz, M. Rospenk, *J. Phys. Chem. A* 107 (2003) 4547–4554.
- [22] M.A. Oturan, J. Peirotten, P. Chartrin, A.J. Acher, *Environ. Sci. Technol.* 34 (2000) 3474–3479.
- [23] C.T. Johnston, G. Sheng, B.J. Teppen, S.A. Boyd, M.F. De Oliveira, *Environ. Sci. Technol.* 36 (2002) 5067–5074.